Measurement 201 (2022) 111744

Contents lists available at ScienceDirect

Measurement

journal homepage: www.elsevier.com/locate/measurement

A versatile wearable based on reconfigurable hardware for biomedical measurements

Víctor Toral [a,*], Francisco J. Romero [b], Encarnación Castillo [a], Diego P. Morales [a], Almudena Rivadeneyra [a], Alfonso Salinas-Castillo [c], Luis Parrilla [a], Antonio García [a]

[a] Dept. Electronics and Computer Technology, University of Granada, 18071 Granada, Spain
[b] Eesy-Innovation Spain S.L., 18014, Granada, Spain
[c] ECsens, Department of Analytical Chemistry, Faculty of Sciences, 18071 University of Granada, Granada, Spain

A B S T R A C T

In this work a versatile hardware platform based on reconfigurable devices is presented. This platform it intended for the acquisition of multiple biosignals, only requiring a reconfiguration to switch applications. This prototype has been combined with graphene-based, flexible electrodes to cover the application to different biosignals presented in this paper, which are electrocardiogram, electrooculogram and electromyogram. The features of this system provide to the user and to medical personnel a complete set of diagnosis tools, available both at home and hospitals, to be used as a triage tool and for remote patient monitoring. Additionally, an Android application has been developed for signal processing and data presentation to the user. The results obtained demonstrate the wide range of possibilities in portable/wearable applications of the combination of reconfigurable devices and flexible electronics, especially for the remote monitoring of patients using multiple biosignals of interest. The versatility of this device makes it a complete set of monitoring tools integrated in a reduced size device.

1. Introduction

Wearable devices have entered in our lives as usual, daily-life complements. The use of smartwatches and wristbands is now almost universal in monitoring activity and sports. However, medical applications are not yet fully supported by these devices. Continuous monitoring, which is the usual aim of wearable devices, is of special interest for chronic conditions such as diabetes or coronary diseases. This continuous monitoring has been usually carried out in hospital facilities or with relatively complex devices like Holter monitors, which can have a considerable impact on the daily life of the user. Furthermore, these devices do not usually provide remote connection or communication with the medical professional requesting the data, so the acquired data have to be processed off-line, after acquisition.

The use of medical wearables is an useful tool to confront the challenge of remote healthcare [1]. This can be useful in many scenarios, ranging from healthcare in spaces with restricted or difficult access, to avoiding saturation of healthcare systems due to ageing population [2,3]. The former will be one of the main challenges for healthcare systems in the future, with an expected noticeable increase of healthcare needs that can be mitigated with remote healthcare technologies [4]. Thanks to the use of wearables, it is possible to displace patient monitoring, or even some treatments, from hospital infrastructures to home environments [5–7]. Home monitoring can also be used either as a triage tool or as preventive diagnosis to determine whether the user requires further treatments and diagnosis tests in a hospital or can be treated at home. To do so, it is needed to have multiple devices available for the different signals required by the medical personnel. The most common biosignals are electrocardiogram (ECG) and electroencephalogram (EEG), but this last one needs of complex devices and controlled conditions for acquisition. Other typical signals are electromyogram (EMG) and electrooculography (EOG). ECG is essential for the detection of cardiovascular conditions such as heart attacks or heart murmurs, which are some of the most common diseases. EMG is used to diagnose motor diseases like muscular dystrophia or myositis, or to monitor chronic motor diseases. EOG is less used than the other two signals and it allows to diagnose retinal abnormalities and attention deficit disorders [8].

Many portable devices for wearable acquisition can be found in the literature, such as ECG [9–13], EMG [14–16] or EEG sensors [17,18]. EOG is a less common application, but still recent works have focused on this topic, as the one proposed by Debbarma *et al.* [19]. However, this kind of systems is designed to acquire only one type of signal or for a concrete application. Several authors have recently worked on the acquisition of multiple signals within a single device, which for many of these works is based on an Application-Specific Integrated Circuit (ASIC) with multiple inputs [20–22]. Other approximation is to use ASICs that

* Corresponding author.
E-mail address: vtoral@ugr.es (V. Toral).

https://doi.org/10.1016/j.measurement.2022.111744
Received 17 May 2022; Received in revised form 26 July 2022; Accepted 7 August 2022
Available online 11 August 2022

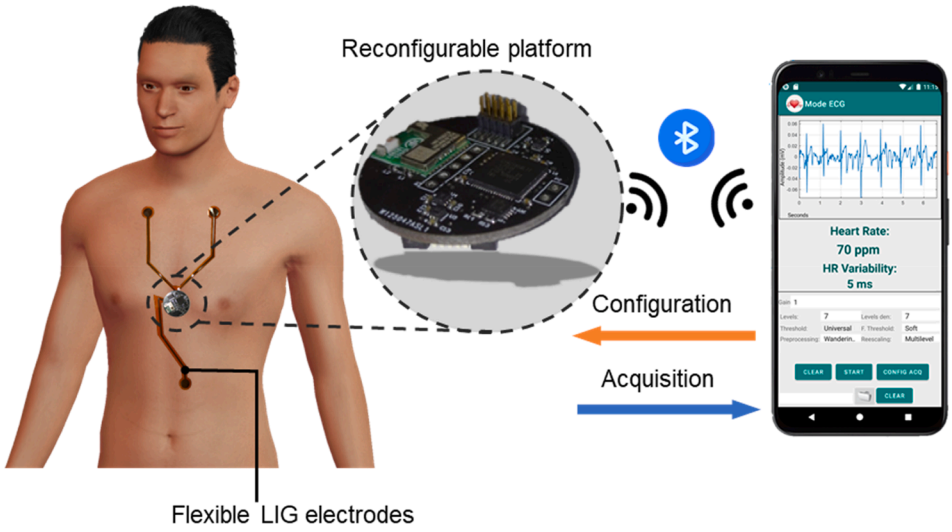

Fig. 1. Conceptual view of the presented system.

provide a reconfigurable front-end rather than multiple inputs, thus allowing to change that front-end and to apply that hardware to different applications [23–25]. Even if this approximation could be adapted to different scenarios, it is still composed of dedicated hardware that cannot be easily modified.

The development of flexible electronics paves the way for new wearable devices that can be better integrated into the daily life of the user [26,27]. Flexible devices are usually based on printed technologies, novel 2D materials, or the combination of these two technologies [28]. The most typical printing technologies are screen and ink-jet printing, along with spray coating [29,30]. For example, ink-jet can be used on textiles to create e-textiles [31], or can be used on flexible substrates to create electrodes for biosignals [32]. These techniques are not limited to electrodes, as they can be also used for temperature or chemical sensors [33–35].

The expansion of 2D materials includes their application to devices for chemical sensing or biosignal acquisition. For example, Soganci *et al.* developed a reduced graphene oxide (rGO) glucose sensor [36]. Also, electrodes can be made of graphene, as those developed by Karim *et al.* [31], Lou *et al.* [37] or Golparvar *et al.* [38] that integrate graphene in textile elements. Laser Induced Graphene (LIG) is also a cost-effective technique to obtain this type of electrodes [32,39,40]. These electrodes have several advantages over the traditional ones, as they are dry and can avoid allergic problems related to pastes used in current alternatives [41–43]. Also polymers are available for these purposes, typically Poli(3,4- Ethylenedioxythiophene)-Poli(Styrene Sulfonate) (PEDOT:PSS) is used alone or in combination with carbon derived materials [44–46].

In this work, we combine the advantages of flexible electronics with analog and digital reconfigurable devices to create a versatile hardware platform able to acquire multiple types of signals, only requiring a reconfiguration to switch applications. This is possible thanks to the reconfiguration capabilities of the presented platform. Combining this feature with flexible electronics makes possible to adapt wearables to different parts of the body, or even integrate them into the user clothing. The device proposed in this paper is able to measure biosignals such as electrocardiogram, electromyogram or electrooculogram with the hardware included in the board and also perform chemical analysis using extension boards and the reconfigurability features of the device. These features provide a complete set of diagnosis tools to the user and to medical personnel, available either at home, to be used as a triage tool, or for remote patient monitoring. Besides, this approach has also several advantages in terms of sustainability. The use of only one device for different purposes allows to reduce electronic waste, reusing the device for different applications [47]. An overview of the system is shown in Fig. 1.

The rest of the manuscript is structured in five sections. Section 2 is devoted to the description of the system and the details of its design. Section 3 details some of the methods used in this work, such as signal acquisition or the definition of some performance parameters. Section 4

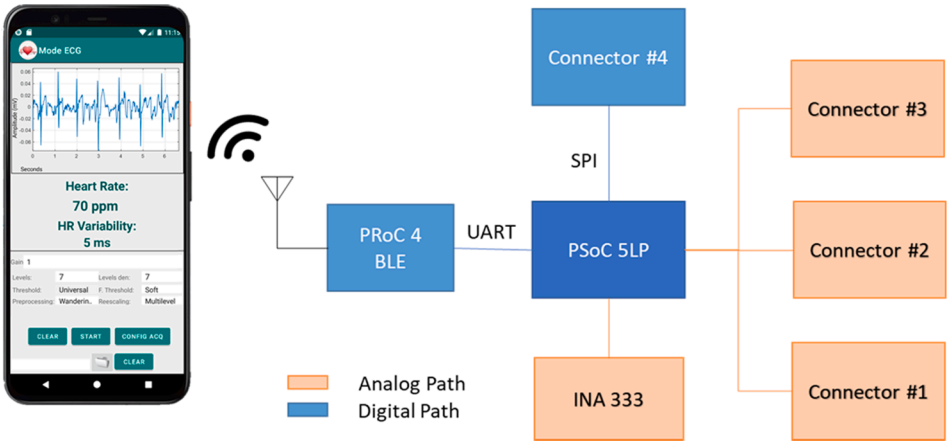

Fig. 2. Schematic view of the developed prototype.

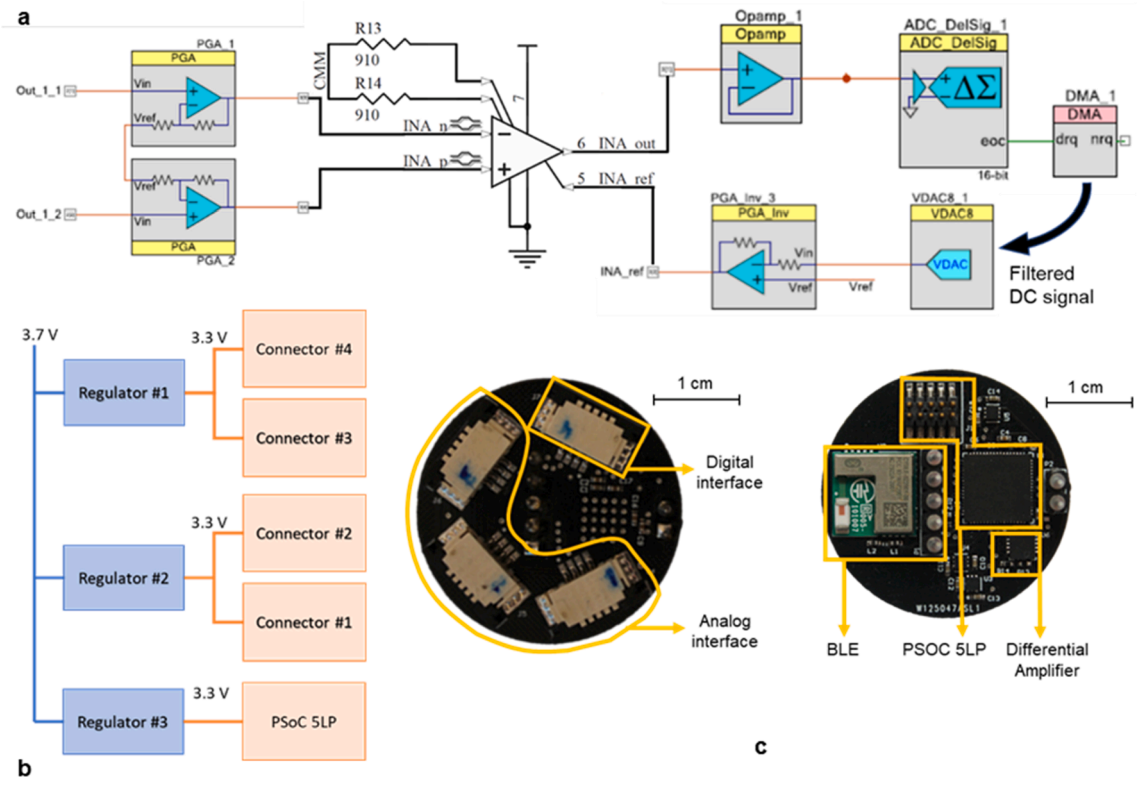

Fig. 3. Proposed system: (a) Detail on the ECG acquisition configuration. (b) Power subsystem scheme. (c) Final prototype.

illustrates the results obtained from the developed prototype. A comparison to other alternatives in the literature is presented in Section 5. Finally, Section 6 summarizes the conclusions derived from this work.

2. System design

2.1. Acquisition system

The developed system is based on reconfigurable devices with analog and digital reconfiguration capabilities, which allow to adapt the acquisition parameters to different biosignals. A schematic overview of the developed system is shown in Fig. 2. The system is based on a Programable System on Chip (PSoC), specifically the PSoc5 LP from Cypress Semiconductors [48]. This unit oversees the interconnection of all the different subsystems thanks to its inherent reconfigurability. The PSoC 5LP also manages communications with external devices through SPI or UART connections. Finally, the Bluetooth connection of the device is controlled by a PSoC4 BLE, also from Cypress Semiconductors [49], which manages the BLE services and communicates data to the central unit. This communication device can be also used to manage auxiliary tasks such as battery monitoring. All connectors referenced in Fig. 2 are flexible, thus allowing to connect either external boards, such as expansion boards, or flexible electrodes or sensors directly linked to the system. These connectors have 4 terminals each one: two of them are power connectors (VCC and GND) and the other two are signal pins. Thanks to this configuration it is possible to connect up to 6 analog signals and 2 digital signals, while 4 power connectors are available in case they are required by any sensor.

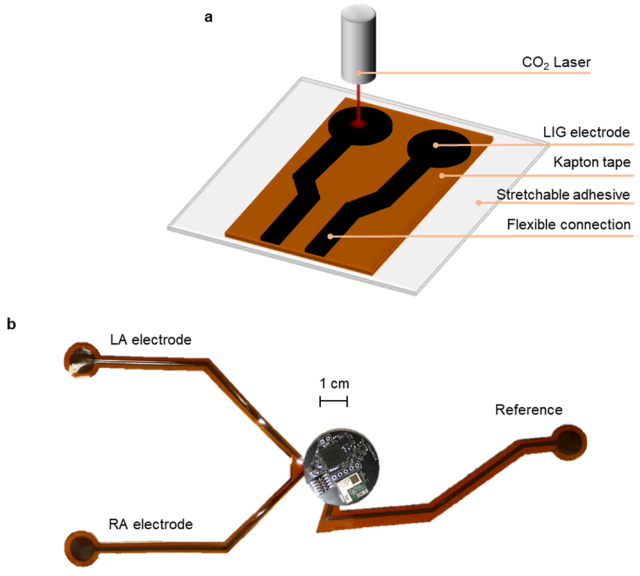

Fig. 4. (a) LIG fabrication process. (b) Electrodes integrated with the prototype.

The system is also equipped with an INA 333 (from Texas Instruments [50]) differential amplifier directly connected to the PSoC5 LP. Thanks to the reconfigurability of the PSoC5 LP, the differential amplifier can be connected to any analog input and combined with the analog circuitry available within the PSoC5 LP. This amplifier has a fixed gain of 50 V/V.

Thanks to the inherent reconfigurability of the PSoC5 LP, the external components can be connected to a variety of different circuits formed by the internal reconfigurable resources in the PSoC5 LP. In Fig. 3a, a representation of the configuration for ECG acquisitions is shown, which exemplifies the philosophy of the developed system in which the INA333 amplifier is connected to two of the inputs through a preamplification stage.

Since the system is oriented to wearable use, power consumption is key. Thus, in order to improve this aspect, different regulators have been included in the device, as it is shown in Fig. 3b. With this, it is possible to power down any external devices not in use. The system can be supplied in the range from 2.0 to 5.5 V, so a wide range of batteries can be used.

Fig. 5. Screenshots of custom Android app.

The system has been tested with a 3.7-V, 350-mAh Li-ion battery that allowed to acquire signals for 16 h. The final appearance of the prototype is shown in Fig. 3c, where the main components are highlighted.

The device is mainly oriented to biosignal acquisition; however, its design also makes it possible to broaden its functionalities to other applications. For example, glucose sensing can be also implemented on this device using the technique presented in [51]. This technique needs of a temperature sensor and a small power supply, so the presented device only requires connecting the temperature sensor to the SPI interface and the heater to one of the available power interfaces. The final processing of this chemical sensor is based on a smartphone through colorimetric measurement.

2.2. Electrodes

The electrodes used in this work are designed with LIG technology, which has been proven to be a cost-efficient option to create flexible electronics [32]. The electrodes are created by laser ablation of Kapton® (Dupont), thus producing the so-called Laser Induced Graphene (LIG). Fig. 4a schematizes the structure of the electrode and its fabrication process. A 2.4-W CO_2 laser is used for the ablation of a Kapton film of 75 μm and, later, an adhesive patch is added to attach the electrode to the skin. The used electrodes are circular, with 1 cm of diameter, which is a size similar to commercial wet electrodes. The skin was only treated cleaning it with alcohol to eliminate any grease or dirt which could affect the measurement. The connections to the board are also imprinted on LIG, thus creating a patch-like electrode that can be used in a completely wearable system, similar to the one presented in [32]. The final aspect of the prototype and the patch electrodes fabricated to acquire ECG signals are shown in Fig. 4b. This image is a clear example of how flexible electrodes, and the presented system can be combined. Just changing the flexible patch and the PSoC5 LP configuration, it is possible to adapt the device to other signals such as EOG or EMG as it is described in Section 3.

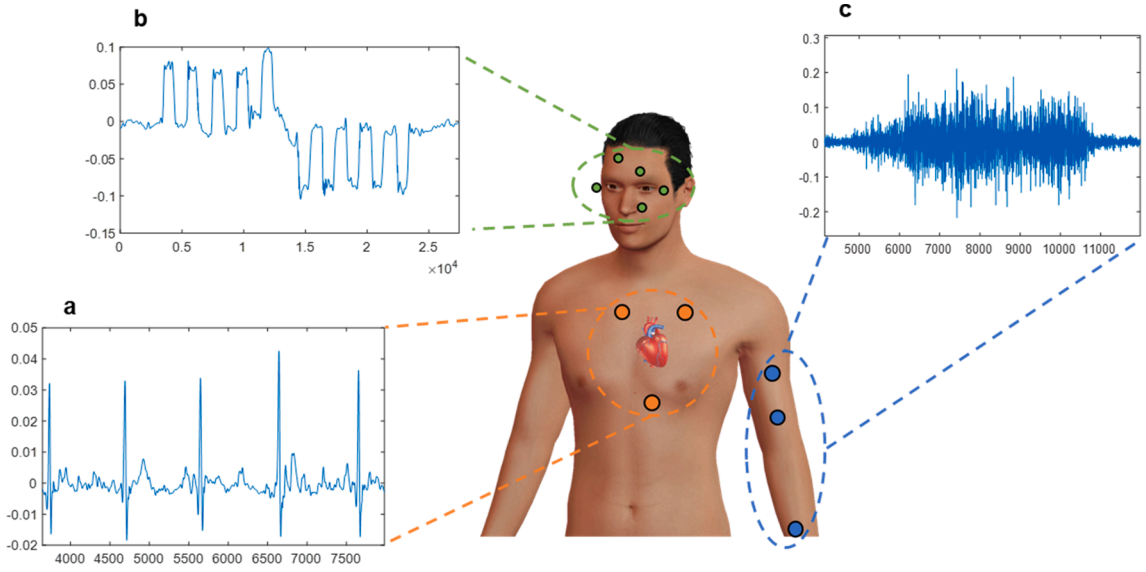

Fig. 6. Acquisition details: (a) ECG signal and placement of electrodes (orange). (b) EOG and placement of electrodes (green). (c) EMG signal and placement of electrodes (blue).

Fig. 7. Position of electrodes in real case uses. (a) EMG acquisition. (b) EOG acquisition. (c) ECG acquisition.

2.3. Android app

A custom Android application has been developed to both configure the system and manage the acquisition of the different biosignals. The app is in charge of configuring the platform, acquiring the signals and processing them. It is also able to store the acquired data in the mobile device. Fig. 5 shows some screenshots of the application. This app has been developed for the API level 31 with Android Studio 4.24 and it is compatible down to API level 26.

The preprocessing of signals to suppress noise and interferences is based on the wavelet transform. To apply this transform to the signals, a high pass filter and low pass filter are applied subsequently to the signal in each of the so-called levels of the transform. The coefficients of the filters depend on the wavelet used for the transform. After the transform, low and high frequency components of the signal are obtained, so it is possible to suppress wandering through the low frequency components and to suppress high-frequency noise over the rest of the signal. As it can be seen in the ECG mode screenshot, the parameters of the signal processing can be changed on the fly to fine tune the algorithm depending on the circumstances of the acquisition. Details on the parameters and the processing can be found in [52]. This method allows to eliminate either wandering or high frequency noise in the case of ECG. For EOG the processing is applied to eliminate high frequency noise. EMG signals are not processed by the app as the filtering applied with the PSoC5 LP is enough for the needs of the subsequent data extraction. Further details on signal processing will be provided in Sections 3 and 4.

3. Methods

In this section the acquisition procedures for different biosignals using the presented prototype will be described. Additionally, details on the signal processing implemented for the different biosignals will be provided, and the performance parameters for each experiment will be presented.

3.1. Acquisition methods

The acquisition of biosignals is carried out with a differential amplification and a reference electrode for common mode and noise cancellation. In the case of ECG signals, Derivation I is acquired on the chest of the user by two electrodes above the heart and the reference electrode below it. The reference electrode is used to provide a common mode of VDD/2, thus allowing the amplifier full swing at the output and the feedback of noise with an inverter amplifier in order to cancel it. The signal is later digitalized at a sampling rate of 1 kHz and filtered with a pass-band filter in the 1–35 Hz band, which includes the main components of the ECG signal. This filter is implemented in the digital configurable part of PSoC5 LP. Fig. 6a represents the positioning of electrodes and an example of the signal obtained from these positions and Fig. 7c shows the actual position of electrodes. With this configuration a set of nine 20-second recordings were acquired from two healthy subjects.

In the case of Electrooculogram (EOG), two channels, vertical and horizontal, are required to track all the eye movements, as illustrated in Fig. 6b. In Fig. 7b the patch-like structure for both channels and the reference is shown in real use. In this case, the signals of both channels are multiplexed to be digitalized by the same Analog-to-Digital Converter (ADC), which samples at 2 kHz in order to digitalize each channel at 1 kHz. As detailed above, the reference is used for noise cancellation and common mode adaption. The filtering in this case is low-pass, with a cut-off frequency of 35 Hz, also implemented in the digital configurable subsystem, since the DC component is required to determine when the eye is fixed at any given position. In order to capture the EOG signal, a guide video (see supporting information) has been used to ensure the same movements were always repeated. The experiments to acquire EOG were focused on the acquisition of the two principal types of eye movement, saccadic and smooth pursuit movements. To achieve this, each acquisition was divided in two parts. In the first one, the subject is asked to make saccadic movements with the eyes looking to a point that suddenly changes its position. These movements are repeated five times in each direction. During the second part of the experiment the user is asked to follow a point that is slowly moving from side to side of the window.

Finally, for EMG signals, the acquisition is carried out in a similar way to that of ECG. However, the spectrum of the EMG signal covers the band between 10 and 300 Hz. Thus, the EMG signal is filtered with a pass-band filter between 10 and 500 Hz. This filter is combined with a notch filter at 50 Hz and 10-Hz bandwidth to suppress electrical grid interferences. The positions of the electrodes are represented in Fig. 6c and shown in real use in Fig. 7a. The acquisition was done during a maximum voluntary isometric contraction test of the brachial bicep. The subject was asked to push, applying the maximum force, against a fixture blocking the arm movement. As it will be detailed in Section 3.2, a commercial instrument for biosignal acquisition, Biosignalsplux [50], is used as a reference for this experiment, which was repeated twice, one acquiring the EMG signals with the proposed prototype and then with the Biosignalsplux device. In the case of this Biosignalsplux device, commercial wet electrodes by Ambu® were used.

3.2. Performance parameters

To analyze the performance of the prototype, several parameters have been defined for each type of biosignal. The parameters are based in the extraction of characteristics of these signals. This way of defining the parameters allows to determine the quality of the acquisition, since a noisy of distorted signal will make more difficult the extraction of any parameters.

In the case of ECG, accuracy in the detection of each heartbeat, also defined as QRS complex for the name of the characteristic's points of each beat, is measured through three parameters, Sensibility, S_e,

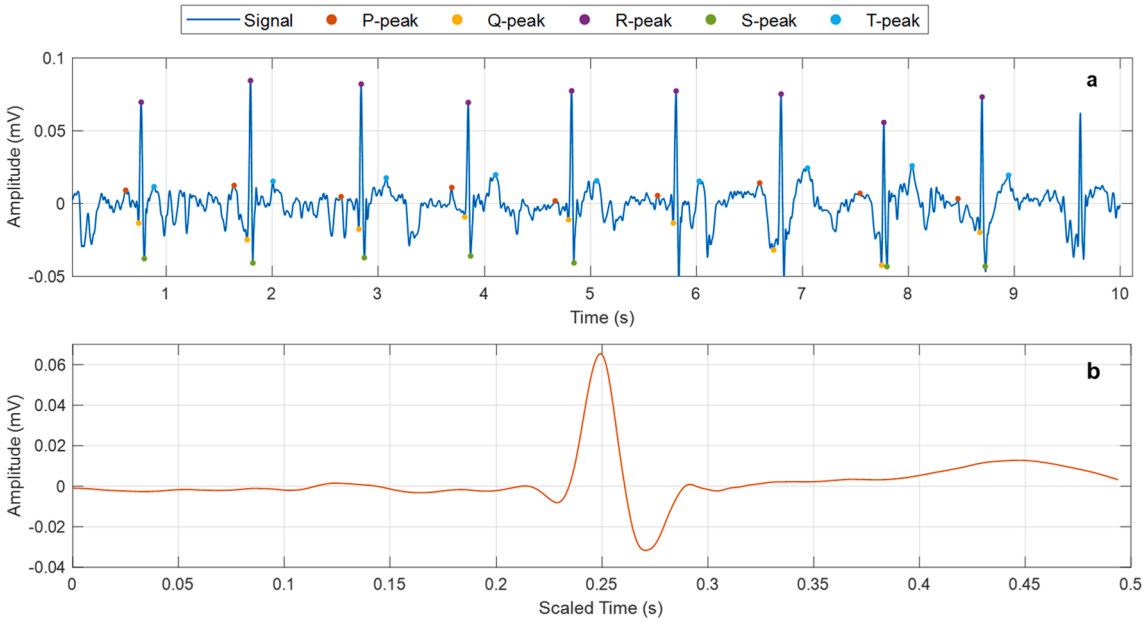

Fig. 8. ECG acquisition. (a) Segment of an ECG signal acquired. (b) Mean QRS complex.

Positive Diagnosis Value, *PDV* and Accuracy, A_{cc}, which are defined as:

$$S_e = \frac{TD}{TD + FN} \tag{1}$$

$$PDV = \frac{TD}{TD + FP} \tag{2}$$

$$A_{cc} = \frac{TD}{TD + FP + FN} \tag{3}$$

where *TD* are the correctly, or true-, detected peaks, *FP* are the False Positives, and *FN* are the False Negatives.

For EOG, the main objective is to determine the direction and amplitude of the movement through the combination of the vertical and horizontal channels, so the error in those directions will be the performance parameter. In this case, the error is defined relative to a deviation of $\pm\frac{\pi}{4}$ from the expected angle of the movement:

$$\varepsilon = \frac{\theta_{\text{expected}} - \theta_{measured}}{\pi/4}$$

Finally, the EMG spectrum is studied obtaining the Mean Frequency (MNF) and Median Frequency (MDF), which have been demonstrated to be useful for analyzing the muscular fatigue during isometric contraction [53,54]. Since in this case it is difficult to determine the correct MNF or MDF of an acquisition, the signals obtained with the proposed instrument will be compared to the obtained with the commercially available Biosignalsplux device, which is specifically designed for biosignal acquisition. Thus, the frequencies obtained with this instrument will be considered as the reference ones and the error in the frequencies obtained from the instrument presented in this work, *MDF*, will be determined as:

$$\varepsilon = \frac{MDF - MDF_{commercial}}{MDF_{commercial}}$$

where $MDF_{commercial}$ is the *MDF* value obtained from the Biosignalsplux device. The same expression for error is considered for the MNF.

4. Results

The results obtained with the presented prototype are illustrated in this section. All the signals have been acquired with the prototype, which transmits the signals in blocks of 5 s through Bluetooth LE to the mobile device. After this transmission, the mobile device processes the signals, which are shown to the user along with the results of the processing.

Table 1
Characteristics of the mean QRS peaks and time segments for the averaged QRS.

Peak	Amplitude (mV)	Standard deviation (mV)	Segment	Length (s)	Standard deviation (s)
P	0.0097	0.0075	**RR**	0.9466	0.0758
Q	−0.0145	0.0140	**PQ**	0.1208	0.0441
R	0.0638	0.0193	**QR**	0.0354	0.0185
S	−0.0376	0.0217	**RS**	0.0255	0.0038
T	0.0182	0.0065	**ST**	0.1927	0.0501

4.1. Electrocardiogram acquisition

The acquisition of ECG signals was done in segments of 20 s and then processed first using wavelet filtering [52] and, subsequently, applying a threshold algorithm to detect the R peaks correspoding to each beat. After that, local minima before and after each R peak are searched for, in order to detect Q and S peaks. Finally, P and T peaks are found by searching for local maxima before Q peaks and after S peaks, respectively. In Fig. 8a, a 10-second segment of one of the acquired ECG signals is shown, including the markers for the PQRST peaks of each beat. As it can be observed, it is possible to detect the characteristic points with a good accuracy for all of Q, R and S points. P and T peaks are more difficult to find, presenting thus higher failure rate in their detections.

Analyzing an averaged QRS-complex, it is possible to more clearly observe the amplitude and timing of each peak, as most of the random noise will be cancelled. Fig. 8b displays the mean QRS-complex obtained from a 20-second recording, which has been obtained after superimposing all detected complexes placing the R-peaks at the reference of the averaged QRS. Using this averaged QRS, the peaks' amplitudes and the duration of the different time segments can be studied. Results in Table 1, obtained from the average QRS in Fig. 8b, show that while Q, R, S and T peaks are cleary appreciable, the P signal presents reduced amplitude and it is hard to distinguish from the noise. Regarding the time segments, the variation is low except for the QR segment, which presents a higher deviation. This can be explained by the low amplitude

Table 2
Performance parameters for ECG signals.

Record	*FN*	*FP*	*TD*	A_{CC}	*PDV*	S_e
ECG_1	1	1	19	90.48%	95.00%	95.00%
ECG_2	1	2	18	85.71%	90.00%	94.74%
ECG_3	2	4	17	73.91%	80.95%	89.47%
ECG_4	1	3	17	80.95%	85.00%	94.44%
ECG_5	1	1	19	90.48%	95.00%	95.00%
ECG_6	3	1	18	81.82%	94.74%	85.71%
ECG_7	1	1	20	90.91%	95.24%	95.24%
ECG_8	1	1	18	90.00%	94.74%	94.74%
ECG_9	1	6	10	58.82%	62.50%	90.91%
		TOTAL	**168**	**82.56%**	**88.13%**	**92.81%**

of the Q peak, which leads to lower precission in its detection along with the typical short duration of this segment, so a small error in the Q-peak determination can be translated into a lage error in the segment determination.

To study FNs and FPs of the obtained ECG records, QRS complexes were manually annotated and the resulting positions compared to those detected with the processing detailed above. As detailed in Section 3.1, the ECG acquistion was carried out with two healthy subjects and 20-second acquisitions for each one. The statitistics, shown in Table 2, were obtained using Eqs. (1)–(3). In general, the system presents an accuracy over 80% along with a similar *PDV*, while S_e is higher and over 90%. Thus, the system detects more false positives than false negatives. This behavior is the usual for threshold detection algorithms in the case of low amplitude signals, since noise can easily be over the threshold. The use of more complex algorithms, such as PCA or clustering methods [55], could improve these results.

4.2. Electrooculogram acquisition

The proposed instrument was also used for EOG acquisition. For this application, two experiments were carried out in order to study the saccadic and pursuit movements while the electrodes were positioned as shown in Fig. 6. An example of the signal obtained from the saccadic movement experiment is shown in Fig. 9. The amplitude in the horizontal channel approximately doubles the vertical channel's since, while the vertical channel captures only one eye, the horizontal captures both. This circumstance has been taken into account when processing the signals.

With these EOG acquisitions, the amplitude of the five movements in each direction has been averaged to estimate the direction and amplitude of movement. In Fig. 10, a vectorial representation of the amplitudes shows the direction and amplitude of movement. The vectors are composed using the amplitudes of each channel (vertical and horizontal) as components of this vector and after normalization to the maximum of them.

With this, it is possible to calculate the error in the determination of direction, as it was detailed in Section 3.2. The results obtained for the precision in the determination of the movement direction are shown in Table 3. As it can be observed, the precision is over 90% in all the cases. The lower precision is obtained for the "look up" movement, which is affected by a blink movement that can be observed in Fig. 9, in the vertical channel. Furthermore, for this movement, the noise amplitude in the horizontal axis is comparable to the signal amplitude of the vertical axis, so this can be confused as actual movements of the eye.

For the study of pursuit movements, the results for both channels are shown in Fig. 11a. In this case, the amplitude of the movement is variable in time. In Fig. 11b, the vectors, obtained as in the case of saccadic movements, are shown over time. Despite the fact these vectors are mainly in the correct direction when the movement is near the peak, there is an appreciable error when the eye is looking ahead (which may be considered as the resting position). In Fig. 11c the angle of sight and the expected angle are represented over time. As Fig. 10c shows, despite the angle being close to the expected value, there is a small constant error, which increases as the direction changes. With all this, the mean error obtained in the experiment is 11% with respect to the expected angle.

4.3. Electromyogram acquisition

The third application of the proposed instrument is the acquisition of EMG signals. As described above, EMG acquisition was carried out on

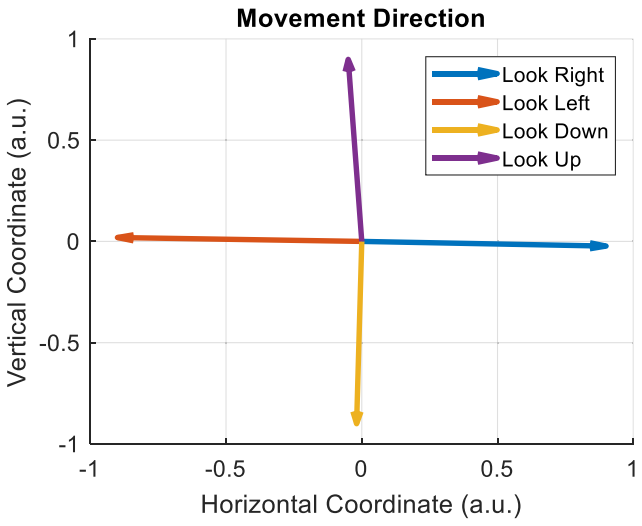

Fig. 10. Estimation of movement directions from EOG signals.

Table 3
Precision in the determination of the direction of the movement.

Look right	Look left	Look down	Look up	Mean	σ
96.7436%	97.2781%	97.3118%	92.9447%	96.0695%	2.0994%

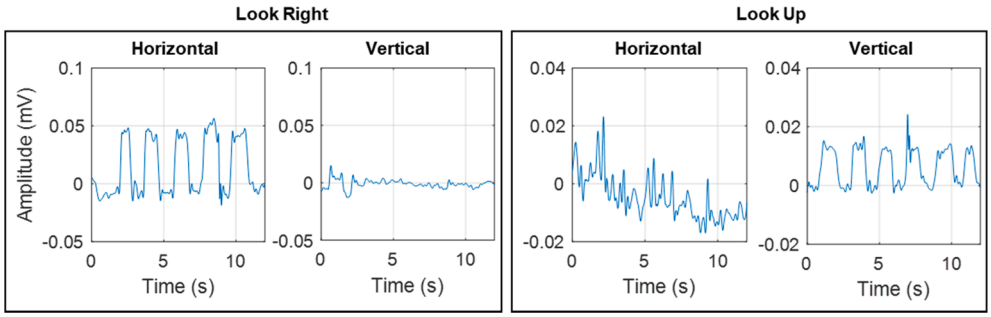

Fig. 9. EOG signals obtained for the Look Right and Look up movements.

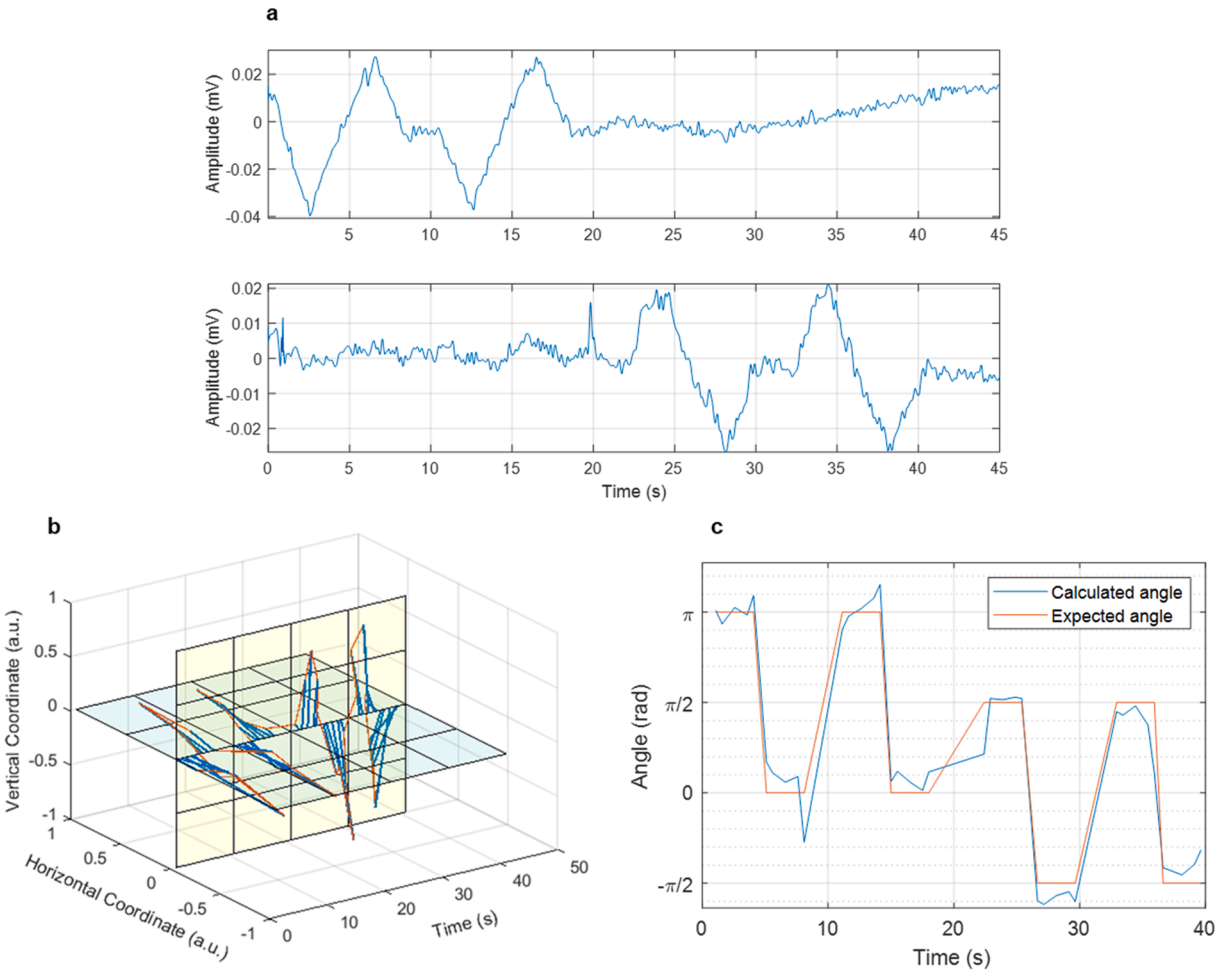

Fig. 11. (a) Acquisition of pursuit movement in horizontal (up) and vertical channels. (b) Vectorial representation in time. (c) Expected and calculated angles form the acquisition.

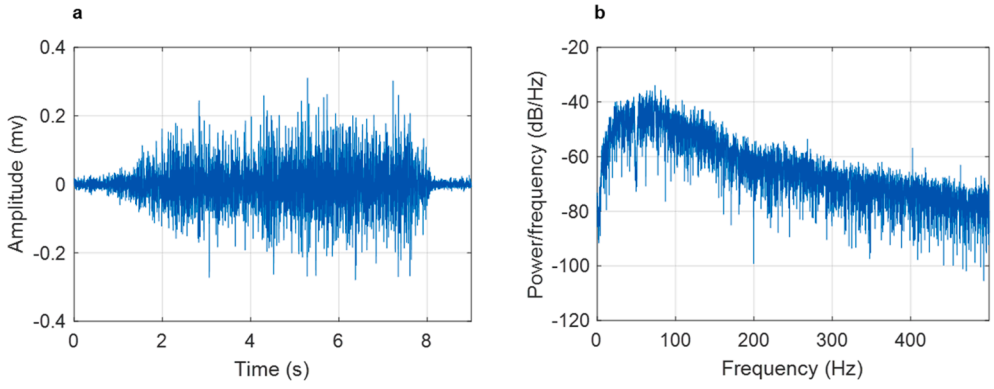

Fig. 12. EMG acquired. (a) EMG signal of an isometric contraction for 6 s. (b) Spectrum of the obtained signal.

Table 4
Results of EMG acquisition.

	MNF (Hz)	MDF (Hz)	RMS (mV)
Prototype instrument	75.24	69.35	0.062
Commercial instrument	65.70	62.44	0.970

the biceps brachii during isometric contraction. The results of this experiment are shown in Fig. 12a. As the parameter of interest for this type of signal is the frequency spectrum, an example of it is shown in Fig. 12b. As it can be observed, the main part of this spectrum is between 30 and 70 Hz.

As detailed in Section 3.2, a Biosignalsplux device was used as reference for this experiment. The frequencies obtained from both Biosignalsplux and the presented instrument are shown in Table 4. The results obtained with Biosignalsplux show lower median and mean frequencies than those from our prototype. Considering the error as detailed in Section 2, the presented device has an error of 14% when compared to the results of Biosignalsplux. This discrepancy may be due to differences in the force exerted by the subject. It is also noticeable a

Table 5
Comparative between recent works and this proposal.

Flexibility	Type of Wearable	Dry/Wet	Interface	Size (mm)	Drawback	Biosignals	Reconfigurability	Ref
No	–	–	Wired	1.7 × 0.6 (chip die)	ASIC	ECG/BioZ/PPG/GPA/GSR	Yes	[24]
Yes	Patch	Dry	Wireless	125 × 18	Not stretchable	EOG	No	[19]
Partial	Patch	Dry	Wireless	3.3 × 3.6	Rigid circuitry	EMG	Yes	[16]
No	–	Wet	Wired	2 × 3 (chip die)	ASIC	PPG/ECG/RR	No	[22]
No	Wristband	Wet	Wireless	40 × 23	ASIC	ECG/PPG/BioZ	No	[21]
No	–	Wet	Wired	1.5 × 1.7 (chip die)	ASIC	ECG/BioZ/RR	No	[20]
No	–	Wet	Wired	5 × 5 (chip die)	ASIC	ECG/PPG	Yes	[23]
Partial	NFC Tag	–	Wired	150 × 70	Specific Tag for each app	ECG/PPG/Temp.	No	[35]
Yes	T-Shirt	Dry	Wireless	Ø 30	Not stretchable	ECG	No	[46]
Partial	Patch	Dry	Wireless	Ø 30	Not stretchable	ECG/EMG/EOG/…	Yes	This work

difference in the RMS value, which can be due to differences in the contact of the electrodes used for both instruments.

5. Comparison to other alternatives

Finally, the presented system and the corresponding results have been compared to several works in the literature [16,19–24,35,46]. Table 5 summarizes a qualitative comparison between some recent works and the current proposal. Two main alternatives can be distinguished in the literature: approaches using an ASIC for several signals, and approaches using a flexible system for a single signal. Some works based on ASICs [20–24], just as this proposal, allow to capture different signals. Unfortunately, they are rigid and, in most cases, do not include the auxiliary hardware needed as power supply or communication subsystems. On the other hand, the approaches based on a device for a specific signal, as those proposed in [19,46], are completely flexible. However, they can only acquire one type of signal and they cannot change their application. The device we propose in this paper combines the advantages of both approaches, *i.e.*, partial flexibility and the ability to acquire multiple signals. In fact, even if the proposed device has only been tested for ECG, EMG and EOG acquisition, it is able to either acquire other signals or switch applications. As an example, this device can be used for some other biological measurements or in chemical sensing, with minimum extra hardware, thanks to its inherent reconfigurability [51].

6. Conclusions

In this paper a new platform intended for the acquisition of biosignals in wearable applications is presented. The proposed prototype makes use of reconfigurable devices to adapt the acquisition interface to different signals, which in combination with flexible low-cost electrodes allow the acquisition of multiple types of signals in a variety of scenarios.

Some of the most common electrical biosignals, such as ECG, EMG and EOG, have been acquired with the presented prototype and LIG electrodes in order to illustrate its capabilities. The performance of this device was remarkable in all the cases studied. For ECG, the accuracy is over 82% in the detection of QRS complexes even when using the most basic detection algorithms. For EOG, it is possible to determine the direction of the movements with an accuracy over 96%. Finally, in the case of EMG, the results showed an error lower than 15% when compared to a commercial *ad hoc* device. When compared to proposals in the literature, in this work we present a device which combines the advantages of different approaches, thus being able to acquire different signals while using flexible electronics to improve ergonomics.

These results demonstrate the wide range of possibilities in portable/wearable applications of the combination of reconfigurable devices with flexible electronics, especially for the remote monitoring of patients using multiple biosignals of interest. Furthermore, this device is not limited to biosignals and its inherent reconfigurability allows it to switch applications in very different fields, for example in portable chemical sensing as described in Section 2.1. The versatility of this device makes it a complete set of monitoring tools integrated in a reduced size device.

CRediT authorship contribution statement

Víctor Toral: Investigation, Validation, Methodology, Software, Writing – original draft. **Francisco J. Romero:** Investigation, Software. **Encarnación Castillo:** Conceptualization, Software, Supervision. **Diego P. Morales:** Conceptualization, Funding acquisition, Supervision. **Almudena Rivadeneyra:** . **Alfonso Salinas-Castillo:** Resources. **Luis Parrilla:** Resources, Supervision, Funding acquisition. **Antonio García:** Supervision, Writing – review & editing, Project administration.

Declaration of Competing Interest

The authors declare that they have no known competing financial interests or personal relationships that could have appeared to influence the work reported in this paper.

Acknowledgments

This work has been supported by the Spanish Ministry of Science and Innovation through the predoctoral grant FPU18/01376 and the project PID2020-117344RB-100, and by FEDER/Junta de Andalucía-Consejería de Transformación Económica, Industria, Conocimiento y Universidades through project PY20-00265.

Appendix A. Supplementary material

Supplementary data to this article can be found online at https://doi.org/10.1016/j.measurement.2022.111744.

References

[1] X. Liang, M. Barua, L.e. Chen, R. Lu, X. Shen, X.u. Li, H. Luo, Enabling pervasive healthcare through continuous remote health monitoring, IEEE Wirel. Commun. 19 (6) (2012) 10–18.
[2] D.P. Morales et al., Wearable biosignal acquisition system for decision aid', May 2018, p. 15. doi: 10.1117/12.2304988.
[3] P. Lloyd-Sherlock, Population ageing in developed and developing regions: implications for health policy, Soc. Sci. Med. 51 (6) (2000) 887–895, https://doi.org/10.1016/S0277-9536(00)00068-X.
[4] M.J. Prince, F. Wu, Y. Guo, L.M. Gutierrez Robledo, M. O'Donnell, R. Sullivan, S. Yusuf, The burden of disease in older people and implications for health policy and practice, Lancet 385 (9967) (2015) 549–562.
[5] J. Navarro, E. Vidaña-Vila, R. Alsina-Pagès, M. Hervás, Real-time distributed architecture for remote acoustic elderly monitoring in residential-scale ambient assisted living scenarios, Sensors 18 (8) (2018) 2492, https://doi.org/10.3390/s18082492.
[6] Minh Pham, Y. Mengistu, Ha Manh Do, Weihua Sheng, Cloud-Based Smart Home Environment (CoSHE) for home healthcare, in: 2016 IEEE International Conference on Automation Science and Engineering (CASE), Fort Worth, TX, USA, Aug. 2016, pp. 483–488. doi: 10.1109/COASE.2016.7743444.
[7] S. Patel, H. Park, P. Bonato, L. Chan, M. Rodgers, A review of wearable sensors and systems with application in rehabilitation, J NeuroEngineering Rehabil 9 (1) (2012) 21, https://doi.org/10.1186/1743-0003-9-21.

[8] F. Latifoğlu, M.Y. Esas, E. Demirci, Diagnosis of attention-deficit hyperactivity disorder using EOG signals: a new approach, Biomed. Eng./Biomed. Tech. 65 (2) (2020) 149–164, https://doi.org/10.1515/bmt-2019-0027.

[9] C. Liu, X. Zhang, L. Zhao, F. Liu, X. Chen, Y. Yao, J. Li, Signal quality assessment and lightweight QRS detection for wearable ECG SmartVest system, IEEE Int. Things J. 6 (2) (2019) 1363–1374.

[10] S. Ramasamy, B. Archana, Wearable sensors for ECG measurement: a review, Sens. Rev. 38 (4) (2018) 412–419, https://doi.org/10.1108/SR-06-2017-0110.

[11] V. Toral, A. García, F. Romero, D. Morales, E. Castillo, L. Parrilla, F. Gómez-Campos, A. Morillas, A. Sánchez, Wearable system for biosignal acquisition and monitoring based on reconfigurable technologies, Sensors 19 (7) (2019) 1590.

[12] G. Cosoli, S. Spinsante, F. Scardulla, L. D'Acquisto, L. Scalise, Wireless ECG and cardiac monitoring systems: State of the art, available commercial devices and useful electronic components, Measurement 177 (2021) 109243, https://doi.org/10.1016/j.measurement.2021.109243.

[13] F. Patlar Akbulut, A. Akan, A smart wearable system for short-term cardiovascular risk assessment with emotional dynamics, Measurement 128 (2018) 237–246.

[14] A. Gruebler, K. Suzuki, Design of a wearable device for reading positive expressions from facial EMG signals, IEEE Trans. Affective Comput. 5 (3) (2014) 227–237, https://doi.org/10.1109/TAFFC.2014.2313557.

[15] R. Di Giminiani, M. Cardinale, M. Ferrari, V. Quaresima, Validation of fabric-based thigh-wearable EMG sensors and oximetry for monitoring quadriceps activity during strength and endurance exercises, Sensors 20 (17) (2020) 4664.

[16] A. Moin et al., An EMG gesture recognition system with flexible high-density sensors and brain-inspired high-dimensional classifier, in: 2018 IEEE International Symposium on Circuits and Systems (ISCAS), Florence, 2018, pp. 1–5. doi: 10.1109/ISCAS.2018.8351613.

[17] G. Li, B.-L. Lee, W.-Y. Chung, Smartwatch-based wearable EEG system for driver drowsiness detection, IEEE Sens. J. 15 (12) (2015) 7169–7180, https://doi.org/10.1109/JSEN.2015.2473679.

[18] M. Ha, S. Lim, H. Ko, Wearable and flexible sensors for user-interactive health-monitoring devices, J. Mater. Chem. B 6 (24) (2018) 4043–4064, https://doi.org/10.1039/C8TB01063C.

[19] S. Debbarma, S. Bhadra, A lightweight flexible wireless electrooculogram monitoring system with printed gold electrodes, IEEE Sens. J. 21 (18) (2021) 20931–20942, https://doi.org/10.1109/JSEN.2021.3095423.

[20] J. Xu, P. Harpe, J. Pettine, C. Van Hoof, and R. F. Yazicioglu, 'A low power configurable bio-impedance spectroscopy (BIS) ASIC with simultaneous ECG and respiration recording functionality, in: ESSCIRC Conference 2015 - 41st European Solid-State Circuits Conference (ESSCIRC), Graz, Austria, September 2015, pp. 396–399. doi: 10.1109/ESSCIRC.2015.7313911.

[21] M. Konijnenburg et al., 28.4 A battery-powered efficient multi-sensor acquisition system with simultaneous ECG, BIO-Z, GSR, and PPG, in: 2016 IEEE International Solid-State Circuits Conference (ISSCC), San Francisco, CA, USA, January 2016, pp. 480–481. doi: 10.1109/ISSCC.2016.7418116.

[22] R. Agarwala, P. Wang, B.H. Calhoun, A 405nW/4.8μW Event-Driven Multi-Modal (V/I/R/C) sensor interface for physiological and environmental co-monitoring, in: 2021 IEEE Biomedical Circuits and Systems Conference (BioCAS), Berlin, Germany, October 2021, pp. 1–4. doi: 10.1109/BioCAS49922.2021.9644963.

[23] J. Kim, H. Ko, Reconfigurable voltage/current readout instrumentation amplifier for cardiovascular health monitoring, in 2018 IEEE International Symposium on Circuits and Systems (ISCAS), Florence, May 2018, pp. 1–4. doi: 10.1109/ISCAS.2018.8350923.

[24] J. Xu, M. Konijnenburg, H. Ha, R. van Wegberg, S. Song, D. Blanco-Almazan, C. Van Hoof, N. Van Helleputte, A 36 μW 1.1 mm ^{2} Reconfigurable analog front-end for cardiovascular and respiratory signals recording, IEEE Trans. Biomed. Circ. Syst. 12 (4) (2018) 774–783.

[25] Y.-J. Huang, T.-H. Tzeng, T.-W. Lin, C.-W. Huang, P.-W. Yen, P.-H. Kuo, C.-T. Lin, S.-S. Lu, A self-powered CMOS reconfigurable multi-sensor SoC for biomedical applications, IEEE J. Solid-State Circ. 49 (4) (2014) 851–866.

[26] W. Gao, H. Ota, D. Kiriya, K. Takei, A. Javey, Flexible electronics toward wearable sensing, Acc. Chem. Res. 52 (3) (2019) 523–533, https://doi.org/10.1021/acs.accounts.8b00500.

[27] Y. Ma, Y. Zhang, S. Cai, Z. Han, X. Liu, F. Wang, Y.u. Cao, Z. Wang, H. Li, Y. Chen, X. Feng, Flexible hybrid electronics for digital healthcare, Adv. Mater. 32 (15) (2020) 1902062.

[28] I.-C. Cheng, S. Wagner, Overview of flexible electronics technology, in: W.S. Wong, A. Salleo (Eds.), Flexible Electronics, vol. 11, Springer US, Boston, MA, 2009, pp. 1–28. doi: 10.1007/978-0-387-74363-9_1.

[29] Z. Cui, Printed Electronics: Materials, Technologies and Applications, Wiley, Singapore, 2016.

[30] S.K. Sinha, Y. Noh, N. Reljin, G.M. Treich, S. Hajeb-Mohammadalipour, Y. Guo, K. H. Chon, G.A. Sotzing, Screen-printed PEDOT:PSS electrodes on commercial finished textiles for electrocardiography, ACS Appl. Mater. Interf. 9 (43) (2017) 37524–37528.

[31] N. Karim, S. Afroj, A. Malandraki, S. Butterworth, C. Beach, M. Rigout, K. S. Novoselov, A.J. Casson, S.G. Yeates, All inkjet-printed graphene-based conductive patterns for wearable e-textile applications, J. Mater. Chem. C 5 (44) (2017) 11640–11648.

[32] V. Toral, E. Castillo, A. Albretch, F.J. Romero, A. Garcia, N. Rodriguez, P. Lugli, D. P. Morales, A. Rivadeneyra, Cost-effective printed electrodes based on emerging materials applied to biosignal acquisition, IEEE Access 8 (2020) 127789–127800.

[33] Y.-F. Wang, T. Sekine, Y. Takeda, K. Yokosawa, H. Matsui, D. Kumaki, T. Shiba, T. Nishikawa, S. Tokito, Fully printed PEDOT:PSS-based temperature sensor with high humidity stability for wireless healthcare monitoring, Sci. Rep. 10 (1) (2020), https://doi.org/10.1038/s41598-020-59432-2.

[34] Y.e. Tang, K. Petropoulos, F. Kurth, H. Gao, D. Migliorelli, O. Guenat, S. Generelli, Screen-printed glucose sensors modified with Cellulose Nanocrystals (CNCs) for cell culture monitoring, Biosensors 10 (9) (2020) 125.

[35] M.S. Zaman, B.I. Morshed, A low-power portable scanner for body-worn Wireless Resistive Analog Passive (WRAP) sensors for mHealth applications, Measurement 177 (2021) 109214, https://doi.org/10.1016/j.measurement.2021.109214.

[36] K. Soganci, H. Bingol, E. Zor, Simply patterned reduced graphene oxide as an effective biosensor platform for glucose determination, J. Electroanal. Chem. 880 (2021) 114801, https://doi.org/10.1016/j.jelechem.2020.114801.

[37] C. Lou, R. Li, Z. Li, T. Liang, Z. Wei, M. Run, X. Yan, X. Liu, Flexible graphene electrodes for prolonged dynamic ECG monitoring, Sensors 16 (11) (2016) 1833.

[38] A.J. Golparvar, M.K. Yapici, Electrooculography by wearable graphene textiles, IEEE Sens. J. 18 (21) (2018) 8971–8978, https://doi.org/10.1109/JSEN.2018.2868879.

[39] B. Sun, R.N. McCay, S. Goswami, Y. Xu, C. Zhang, Y. Ling, J. Lin, Z. Yan, Gas-permeable, multifunctional on-skin electronics based on laser-induced porous graphene and sugar-templated elastomer sponges, Adv. Mater. 30 (50) (2018) 1804327.

[40] F.J. Romero, E. Castillo, A. Rivadeneyra, A. Toral-Lopez, M. Becherer, F.G. Ruiz, N. Rodriguez, D.P. Morales, Inexpensive and flexible nanographene-based electrodes for ubiquitous electrocardiogram monitoring, NPJ Flex Electron. 3 (1) (2019).

[41] R.J. Cochran, THEODORE Rosen, Contact dermatitis caused by ECG electrode paste: South. Med. J. 73 (12) (1980) 1667–1668.

[42] Y.M. Chi, T.-P. Jung, G. Cauwenberghs, Dry-contact and noncontact biopotential electrodes: methodological review, IEEE Rev. Biomed. Eng. 3 (2010) 106–119, https://doi.org/10.1109/RBME.2010.2084078.

[43] W. Uter, H.J. Schwanitz, Contact dermatitis from propylene glycol in ECG electrode gel, Contact Dermat. 34 (3) (1996) 230–231, https://doi.org/10.1111/j.1600-0536.1996.tb02190.x.

[44] J. Roopa, K.S. Geetha, B.S. Satyanarayana, Fabrication of polymer based flexible sensors for EoG and EMG applications, S2214785321059265, Mater. Today:. Proc. (2021), https://doi.org/10.1016/j.matpr.2021.09.129.

[45] C.-Y. Huang, C.-W. Chiu, Facile fabrication of a stretchable and flexible nanofiber carbon film-sensing electrode by electrospinning and its application in smart clothing for ECG and EMG monitoring, ACS Appl. Electron. Mater. 3 (2) (Feb. 2021) 676–686, https://doi.org/10.1021/acsaelm.0c00841.

[46] S. Masihi, M. Panahi, D. Maddipatla, A.J. Hanson, S. Fenech, L. Bonek, N. Sapoznik, P.D. Fleming, B.J. Bazuin, M.Z. Atashbar, Development of a flexible wireless ECG monitoring device with dry fabric electrodes for wearable applications, IEEE Sens. J. 22 (12) (2022) 11223–11232.

[47] V. Toral-López, C. González, F.J. Romero, E. Castillo, L. Parrilla, A. García, N. Rodriguez, A. Rivadeneyra, D.P. Morales, Reconfigurable electronics: addressing the uncontrolled increase of waste electrical and electronic equipment, Resour. Conserv. Recycl. 138 (2018) 47–48.

[48] Cypress Semiconductors Corporation, *PSoC 5 LP Family Datasheet*. 2016. [Online]. <http://www.cypress.com/file/45906/download>.

[49] Cypress, 'CYBLE-214015-01 EZ-BLE^{TM} Creator Module'. [Online]. <https://www.mouser.es/datasheet/2/100/CYPR_S_A0011803837_1-2541406.pdf>.

[50] Texas Instruments, 'INA333 Micro-Power (50μA), Zerø-Drift, Rail-to-Rail Out Instrumentation Amplifier'. Dec. 2015. [Online]. <https://www.ti.com/lit/ds/symlink/ina333.pdf?ts=1651493600551&ref_url=https%253A%252F%252Fwww.google.com%252F>.

[51] I. Ortiz-Gómez, V. Toral-López, F.J. Romero, I. de Orbe-Payá, A. García, N. Rodríguez, L.F. Capitán-Vallvey, D.P. Morales, A. Salinas-Castillo, In situ synthesis of fluorescent silicon nanodots for determination of total carbohydrates in a paper microfluidic device combined with laser prepared graphene heater, Sens. Actuat., B 332 (2021) 129506.

[52] E. Castillo, D.P. Morales, A. García, F. Martínez-Martí, L. Parrilla, A.J. Palma, Noise suppression in ECG signals through efficient one-step wavelet processing techniques, J. Appl. Math. 2013 (2013) 1–13.

[53] D. Meldrum, E. Cahalane, R. Conroy, D. Fitzgerald, O. Hardiman, Maximum voluntary isometric contraction: reference values and clinical application, Amyotroph. Later. Scleros. 8 (1) (2007) 47–55, https://doi.org/10.1080/17482960601012491.

[54] L. Qi, J.M. Wakeling, A. Green, K. Lambrecht, M. Ferguson-Pell, Spectral properties of electromyographic and mechanomyographic signals during isometric ramp and step contractions in biceps brachii, J. Electromyogr. Kinesiol. 21 (1) (2011) 128–135, https://doi.org/10.1016/j.jelekin.2010.09.006.

[55] E. Castillo, D.P. Morales, A. García, L. Parrilla, V.U. Ruiz, J.A. Álvarez-Bermejo, E. G. Tolkacheva, A clustering-based method for single-channel fetal heart rate monitoring, PLoS ONE 13 (6) (2018) e0199308.